RESEARCH ARTICLE

Hugo Merchant · Alexandra Battaglia-Mayer ·
Apostolos P. Georgopoulos

Decoding of path-guided apparent motion from neural ensembles in posterior parietal cortex

Abstract We compared quantitatively the psychometric capacity of human subjects to detect path-guided apparent motion (PAM) and the accuracy of cell ensembles in area 7a to code the same type of stimuli. Nine human subjects performed a detection task of PAM. They were instructed to indicate with a key-press whether they perceived a circularly moving object when five stimuli were flashed successively at the vertices of a regular pentagon. The stimuli were presented along a low contrast circular path with one of 33 speeds (150–600°/s). The average psychometric curve revealed that the threshold for PAM detection was 314°/s. The minimum and maximum thresholds for individual subjects were 277° and 378°/s, respectively. In addition, the activity of cells in area 7a that were modulated by the stimulus position in real or apparent motion was used in a multivariate linear regression analysis to recover the stimulus position over time. Real stimulus motion was decoded successfully from neural ensemble activity at all speeds. In contrast, the decoding of PAM was poor at low stimulus speeds but improved markedly above 300°/s: in fact, this was very close to the threshold above for human subjects to perceive continuous stimulus motion in this condition. These results suggest that the posterior parietal cortex is part of a high-level system that is directly involved in the dynamic representation of complex motion

H. Merchant (✉) · A. Battaglia-Mayer · A. P. Georgopoulos
Department of Neuroscience, University of Minnesota,
Minneapolis, MN, 55455, USA
e-mail: merch006@umn.edu
Tel.: +1-552-56234040
Fax: 1-552-56234005

H. Merchant · A. Battaglia-Mayer · A. P. Georgopoulos
Brain Sciences Center, Veterans Affairs Medical Center,
Minneapolis, MN, 55417, USA

Present address:
H. Merchant
Instituto de Neurobiología UNAM, Campus Juriquilla,
76230 Querétaro, Qro, Mexico

Introduction

When an object is flashing with the appropriate timing and spatial distance, the visual system creates a motion percept (called apparent motion) that reflects a built-in knowledge of the properties of the physical world (Anstis 1980; Shepard 1984). Experimental psychologists have studied this phenomenon for more than a century, determining the physical properties of intermittent stimuli that can produce the "fill-in" process associated with motion perception. A wide variety of stimuli has been used, ranging from flashing bars to alternating photographs of the human body in different positions (Chatterjee et al. 1996; Kolers 1972; Ramachandran and Anstis 1983). An example of a complex motion percept is the path-guided apparent motion (Shepard and Zare 1983; Yantis and Nakama 1998). This type of apparent motion is produced when a curved gray path is flashed between two alternately displayed black dots, which create a strong illusion of a single dot moving back and forth along that path. In fact under this condition the interstimulus interval (ISI) necessary to produce an apparent motion illusion increases linearly with the length of the path (Shepard and Zare 1983).

Many neurophysiological studies have used apparent motion to investigate the neural mechanisms underlying the critical features of the stimulus that can produce a motion percept. Cells in the middle temporal area (MT) respond selectively to the direction of visual motion. This directional selectivity is maintained when bars are flashed with the ISI and spatial separation that give rise to apparent motion perception (Mikami 1991; Newsome et al. 1986). In addition, functional magnetic resonance imaging studies have demonstrated that the MT human homolog (hMT[+]) is activated when apparent motion is perceived (Muckli et al. 2002; Sterzer et al. 2002). Nevertheless MT is only one node of a distributed system

engaged in visual motion that involves also the medial superior temporal area and various areas of the posterior parietal cortex, including the lateral intraparietal area, ventral intraparietal area, and area 7a (Andersen et al. 1990; Felleman and Van Essen 1991). Recently it was found that the activity of direction selective cells in three visual motion areas can predict the perceived direction of complex perceptually bistable apparent motion stimuli (Williams et al. 2003). However, these cells were more common in the lateral intraparietal area, less common in the medial superior temporal area, and practically nonexistent in MT. This pattern suggests that the neural activity is better correlated with the perception of complex apparent motion in higher parietal areas, which fits in with the anatomical hierarchy of these areas in the parietal visual stream (Andersen et al. 1990). These experiments support a late instead of an early cortical locus for the perceptual filling-in during apparent motion (Liu et al. 2004). In fact psychophysical as well as lesion studies have suggested that motion perception depends on two motion systems. A low level system that is effortless and passive, and which probably depends on the activity of neurons in V1 and MT, and a high level system that requires attention and has been linked to posterior parietal areas (Batelli et al. 2001; Cavanagh 1992; Lu and Sperling 2001).

In the present study we sought to determine the capabilities of ensembles of neurons in area 7a to decode continuous circularly moving stimuli as well as the perceptual reconstruction of path-guided apparent motion stimuli with a circular path. The hypothesis here was that the fidelity of population representation of circular motion in area 7a should be strictly linked to the perception of real and path-guided apparent circular motion. The results showed, first, that populations of area 7a cells can accurately reconstruct the circular trajectory of real moving stimuli for the range of speeds tested. In addition, we found a tight correlation between the neurophysiological and psychophysical responses to path-guided apparent motion, in that the ISI for detection of path-guided apparent motion in human subjects was similar to the ISI at which neural ensembles decoded properly the perceptual reconstruction of the stimulus.

Materials and methods

Psychophysics in human subjects

Nine healthy human subjects (two women, seven men; age range 24–44 years) participated in this experiment as volunteers. Subjects had normal or corrected visual acuity. The experimental protocol was approved by the institutional review board, and informed consent was obtained. The subjects' informed consent was obtained according to the Declaration of Helsinki.

Visual display

A computer color monitor (Gateway2000 model Crystalscan 1024) was used to display the visual stimuli. It was placed 57 cm in front of the subjects and run at a 60 Hz refresh rate; 1 cm on the screen subtended approximately 1° of visual angle. The apparent moving stimuli consisted of black circles (1.7 cm in diameter) that were flashed successively for 16.7 ms, at the vertices of a regular pentagon. The stimuli were presented on a low contrast circular annulus of 15.2 cm outside diameter and 1.7 cm width. Thirty-three ISIs (the period between the onsets of consecutive stimuli) were used, ranging from 120 to 480 ms and corresponding to a stimulus speed of 150–600°/s. All the stimuli traveled counterclockwise and the starting point was 0° (3 o'clock).

Apparatus and behavioral task

The subjects pressed one of two keyboard buttons to indicate whether the stimulus was moving with apparent motion. At the beginning of the trial a fixation point (0.5 cm in diameter) was presented in the center of the low contrast path, and then after a delay period (300 ms) the stimulus began to move. The subject pushed the key no. 1 to indicate apparent motion perception, considered as smooth motion of the stimulus across the low contrast path, or the key no. 2 instead, to indicate that the stimulus was perceived as a jumping dot illuminated sequentially in an interrupted fashion at the vertices of the pentagon. Subjects were instructed to fixate the FP, although the eye position was not recorded. In addition no time constrains were imposed on the subjects to indicate their perceptual decision. All possible stimulus speeds were presented in a pseudorandom order inside a repetition. Ten repetitions were collected in each subject. Several practice trails were performed before the actual collection.

Neurophysiological experiments in monkeys

Experiments were performed in two male monkeys (*Macaca mulatta*, 4 and 7 kg BW). Impulse activity of single neurons was recorded extracellularly from the left area 7a (for details see Merchant et al. 2001). Animal care conformed to the principles outlined in the Guide for Care and Use of Laboratory Animals (National Institutes for Health publication no. 85-23, revised 1985). The experimental protocol was approved by the institutional review board.

Visual stimuli

The stimuli were back-projected on a tangent screen using an LCD projector (NEC Multisync MT 820/1020). The tangent screen was 69×69 cm and was placed 48.5 cm in front of the animal. The moving stimulus was a black

circle of 1.44 cm [1.7° of visual angle (DVA)], and traveled on a low contrast circular annulus of 15.2 DVA outside diameter and 1.7 DVA width (Fig. 1). The stimuli could move in the real or the apparent motion conditions (Fig. 1A) with one of five angular velocities: 180, 300, 420, 480, and 540°/s. In the real motion condition the stimulus was displayed every 16.7 ms, resulting in a smooth stimulus motion, which was indistinguishable from a continuously moving stimulus. In the apparent motion condition five stimuli were flashed successively for 16.7 ms at the vertices of a regular pentagon. The ISI in this condition was 400, 240, 166.6, 150, and 133.4 ms for the speed of 180, 300, 420, 480, and 540°/s, respectively. All the stimuli traveled counterclockwise.

Task

Monkeys were seated in a primate chair with the left arm loosely restrained, and operated a semi-isometric joystick (Measurement Systems, Model 467-G824, Norwalk Conn., USA) with the right arm. This joystick was a
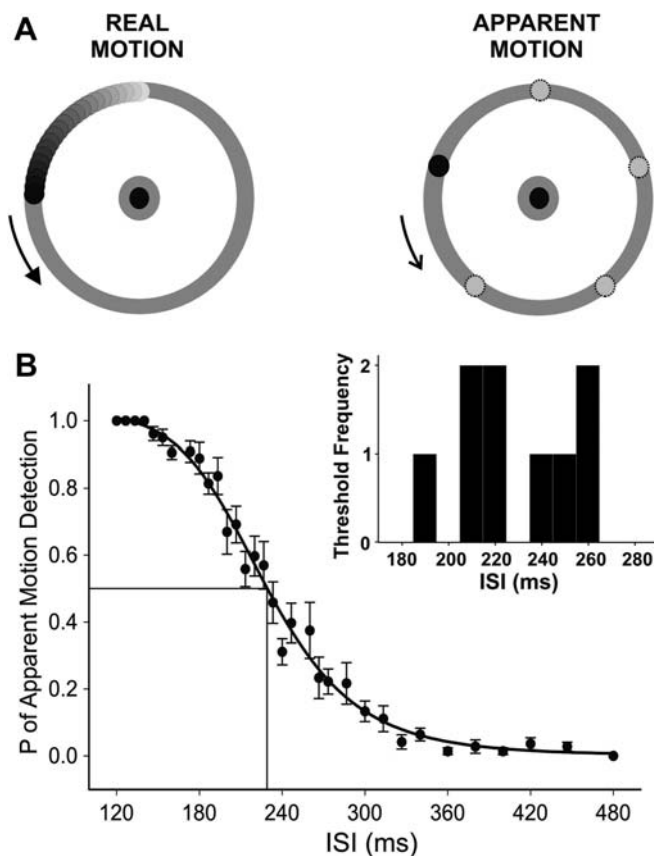

Fig. 1 A Stimuli in the real and apparent motion conditions. A smooth real moving stimulus was produced in the real motion condition. In the apparent motion condition five stimuli were flashed at the vertices of a regular pentagon. All stimuli traveled counterclockwise, through a circular low contrast path. **B** Psychometric curve of apparent motion detection (mean ±SD) using the performance of nine human subjects for 33 different ISIs. The inset shows the distribution of apparent motion detection thresholds (P=0.5) for individual subjects

vertical rod placed in front of the animal and controlled a net force feedback cursor which was displayed in the monitor as a circle of 1.7 DVA in diameter. The feedback cursor was deflected constantly by 1.7 DVA upward to simulate a bias force of 0.108 N. At the beginning of the trial, the animal had to place the force feedback cursor within a red circle of 3.4 DVA in diameter ("center window," located at the center of the screen) by exerting a minimum of 0.108 N in the downward direction, and to keep it there for a variable delay period (1–3 s). After the delay period the stimulus began to move for 2 s. Monkeys received a liquid reward if the cursor was maintained inside the center window throughout the entire duration of the trial. The monkeys were trained to fixate within 2 DVA a yellow dot (1 DVA in diameter) located in the center of the center window for the duration of stimulus presentation. Thus the arm and eye position were constrained during the stimulus presentation. The x-y eye position was monitored using an oculometer (Dr. Bouis, Karlsruhe, Germany). Both the eye and the joystick positions were sampled at 200 Hz. The different combinations of stimulus speeds and motion conditions were interleaved and presented in a pseudorandom order. A repetition consisted of five trials in the real and five trials in the apparent motion condition. At least five repetitions were collected.

Data analysis

Cell Tuning

The preferred stimulus angular location for each cell was computed as follows (see Merchant et al. 2004a). First, an angle was assigned to each action potential during the visual stimulation period. This angle corresponded to the actual (real motion) or the "illusory" (apparent motion) stimulus location in the circular path when the action potential occurred. Figure 2B illustrates a typical example of a spatiotemporal circular raster. The second step was to compute the mean direction using the angles assigned to each action potential. Finally, we used a bootstrapping technique to determine whether the cells were significantly tuned to the stimulus location. For this purpose the length of the mean resultant ($\overline{R}$) was calculated first using the data of the five repetitions collected. Then a bootstrap sample was generated by assigning randomly a new angle (with replacement) to each action potential recorded during the analyzed stimulus revolution, and its mean resultant $\overline{R}^{*}$ R^{*} calculated. A cell was considered to be significantly tuned to the stimulus location if the discharge rate during first revolution was larger than 10 spikes/s and the length of R was greater than 95% of the lengths of R^{*} (k=5000 bootstrap samples). This corresponded to a chance probability of $P<0.05$.

Fig. 2 A Discharge rate (mean ±SEM) of 90 neurons that were tuned to the stimulus position in the real motion condition plotted as a function of the stimulus angle centered at preferred direction of each cell. The discharge rate is computed every 20 ms bins for all the stimulus speeds. **B** Circular raster of the activity of a tuned neuron in area 7a. An angle was assigned to each action potential during the visual stimulation period. This angle corresponded to the actual stimulus location in the circular path when the action potential was recorded (see Merchant et al. 2004a for more details). **C** Preferred angular positions of the 90 cells

Real Motion

Apparent Motion

180   300   420   480   540
Degrees/s
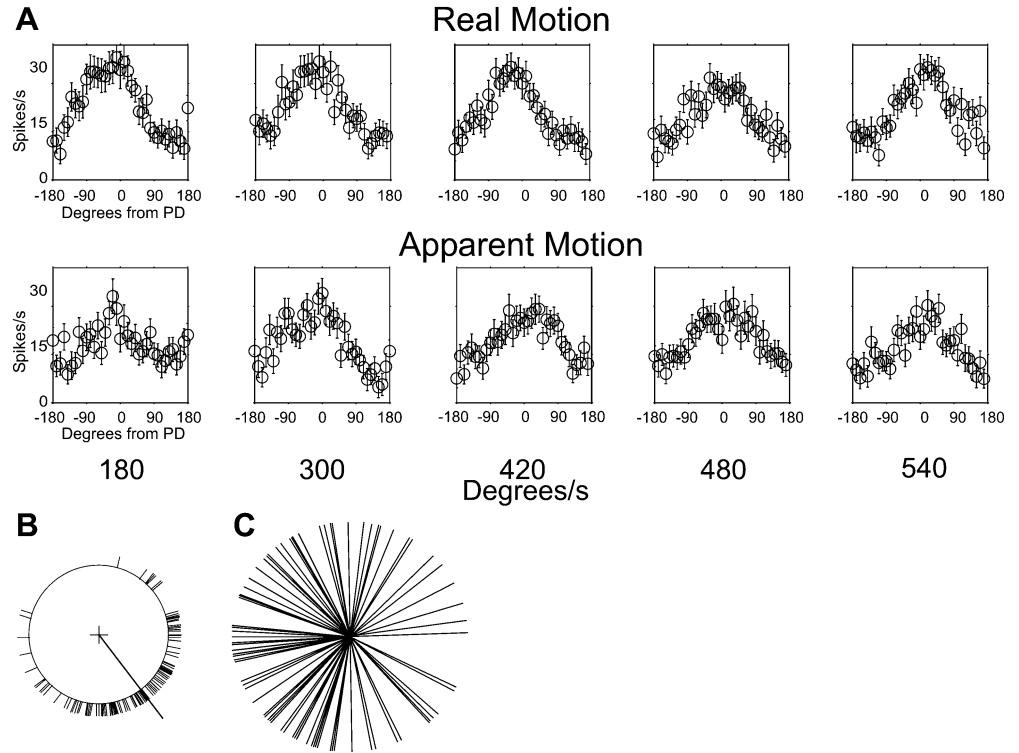
Multivariate multiple linear regression for the stimulus position

We used a linear system analysis to estimate the "true" value of the stimulus position over time on the basis of the discharge rate of cell populations tuned to the stimulus angular position. The regression model that was used for the reconstruction of the stimulus location in real motion, using the activity of a population of cells was the following:

$$R_{x,y(t_k)} = b + \sum_{i=l}^{N} \sum_{j=0}^{\tau} A_{ij} V_i \left(t_{k-j} - \delta \right) + \varepsilon_{t_k} \tag{1}$$

where R is the cosine (x) or sine (y) of the stimulus angle, b is a constant, N is the number of analyzed neurons, τ is the time length (width) of the kernel window, A are the coefficients of the regression that define the kernel, t_k is a specific time period of visual stimulation (binned every 15 ms), and δ is the time lag between t_k and the beginning of τ, and V is an estimate of the instantaneous firing rate at the time $t_k - \delta$. Finally, ε_{tk} is the error term. This equation defines a linear system that determines the coefficients of the transfer function or kernel A. When A is convolved with the spike trains V, the result is an estimate of the x and y components of the stimulus position R.

For the real motion condition we used a cross-validation (leave-one-out) method to determine the validity of the regression models using different time lags (δ), kernel window durations (τ), and number of neurons in the model (N). This method avoided overfitting and consisted of

finding the coefficients of the regression of Eq. 1 using four of the five trials recorded for a particular stimulus speed. Then the regression was solved using the neural activity of the trial that was removed and the sum of squared errors (SSE) was estimated as follows:

SSE

$$= \sum_t \left(R_x(t) - \hat{\hat{R}}_x(t) \right)^2 + \sum_t \left(R_y(t) - \hat{\hat{R}}_y(t) \right)^2 \tag{2}$$

where R_x is the cosine of the stimulus angle and $\hat{\hat{R}}_x$ is the predicted stimulus position in the x dimension, and the subscript y in the second term of the equation correspond to the stimulus position in the y dimension. In addition, the total sum of squares (SST) was calculated as:

SST

$$= \sum_t \left(R_x(t) - \bar{\bar{R}}_x(t) \right)^2 + \sum_t \left(R_y(t) - \bar{\bar{R}}_y(t) \right)^2 \tag{3}$$

where $\bar{\bar{R}}_x$ is the mean stimulus position in the x dimension and $\bar{\bar{R}}_y$ is the mean stimulus position in the y dimension. This procedure was carried out for each trial in the data set, accumulating the *SSE* and the *SST* for a total of five five iterations. The coefficient of determination (R^2) then was calculated as:

$$R^2 = \frac{SST - SSE}{SST} \tag{4}$$

This computation of R^2 is approximately the average R^2 of the regression models with a single trial left out, is very robust to overfitting, and controls the bias variance trade-off effectively.

For the apparent motion condition, first, we estimated the coefficients A of the regression model in Eq. 1 using the activity of an ensemble of neurons during the five trials of real motion for a particular stimulus speed. Then the regression was solved using the neural activity recorded during the five trials of apparent motion and the SSE, SST, and R^2 were calculated.

Results

Path-guided apparent motion detection

In order to establish the detection threshold for path-guided apparent motion perception in human subjects we varied the ISI of dots flashing consecutively at the vertices of a regular pentagon (Fig. 1). These stimuli were presented on a low contrast circular annulus in order to produce path-guided apparent motion along the circular path. A psychometric function was calculated by plotting the probability of apparent motion detection as a function of the ISI for each subject, and a sigmoidal regression was fitted to these data. The distribution of ISI thresholds (at $P=0.5$) is showed in the inset of Fig. 1B and indicated that despite the intersubject variability the ISI threshold was close to 220 ms. In fact the ISI detection threshold obtained from the all-subject mean psychometric curve was 229.3 ms (Fig. 1B), which corresponds to a stimulus speed threshold of 314°/s (since the distance between dots was kept constant).

Neural coding of stimulus position

Our database consisted of 780 cells in area 7a that fulfilled the criteria for number of trials and strength of responses during the task (see Merchant et al. 2004a). The analysis described below was performed on an ensemble of 90 (90/780, 11.5%) cells, the activity of which was significantly modulated by the stimulus position during

Table 1 Number of significantly tuned cells for the noted stimulus speeds in the real and apparent motion condition

Stimulus speed	Real motion	Apparent motion
180	64	55
300	66	59
420	68	54
480	64	63
540	68	58

the task in both motion conditions (see "Methods"). Specifically, these neurons showed at least one significant preferred angular position for a stimulus speed in the real and the apparent motion conditions. Table 1 shows that in this ensemble more than 50 neurons were significantly tuned to the angular position in all combinations of stimulus speeds and motion conditions. Figure 2 shows the discharge rate (mean ± SEM) of these neurons as a function of the stimulus angle centered at the preferred angle for each cell. The neural activity was clearly tuned to the stimulus angle in both motion conditions and all the stimulus speeds. In addition, the distribution of preferred directions was evenly distributed, although slightly skewed to the left (contralateral hemifield) in this neural population (Fig. 2C). Figure 3 shows a typical example of a neuron tuned to the stimulus angle in both motion conditions. An extensive description of the basic physiological properties of these neurons, including receptive field position and size, directional, and velocity selectivity, and responses to rectilinear stimuli is published elsewhere (Merchant et al. 2001, 2004a).

The main purpose of this study was to estimate the circularly moving position of the stimulus on the basis of the spike activity of population of cells tuned to the stimulus angular position. To this end the neuronal activity was analyzed using a multivariate linear regression model (Wessberg et al. 2000). This analysis was designed to find a transfer function or kernel which, when convolved with the spike trains of the population, would provide an estimate of the stimulus position over time. The predicted stimulus position using a particular cell ensemble is depicted in Fig. 4. The stimulus reconstruction was very accurate for all stimulus speeds in the real motion condition. In contrast, in the apparent motion situation

Fig. 3 Circular raster of a neuron with a significant preferred stimulus angular location (PSAL) in all stimulus speeds in the real motion condition and with a significant PSAL in the fastest stimulus speeds in the apparent motion condition. The vector from the center cross to the circular raster represents the significant PSAL (for more details see Merchant et al. 2004a)
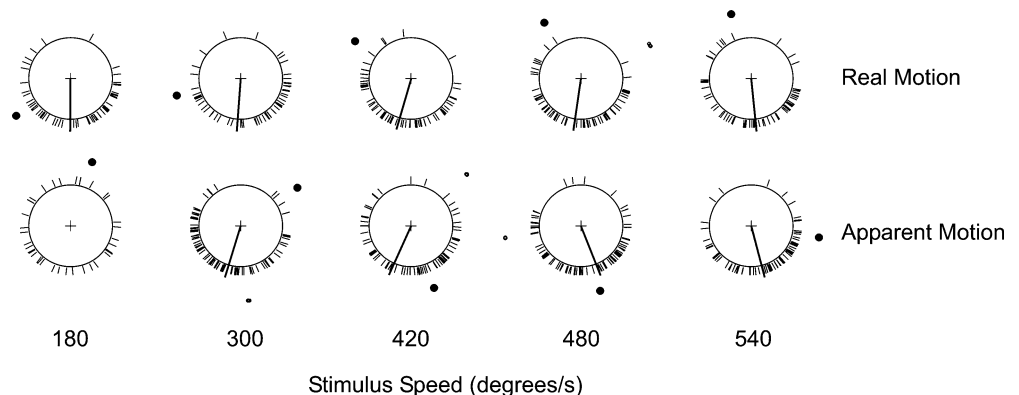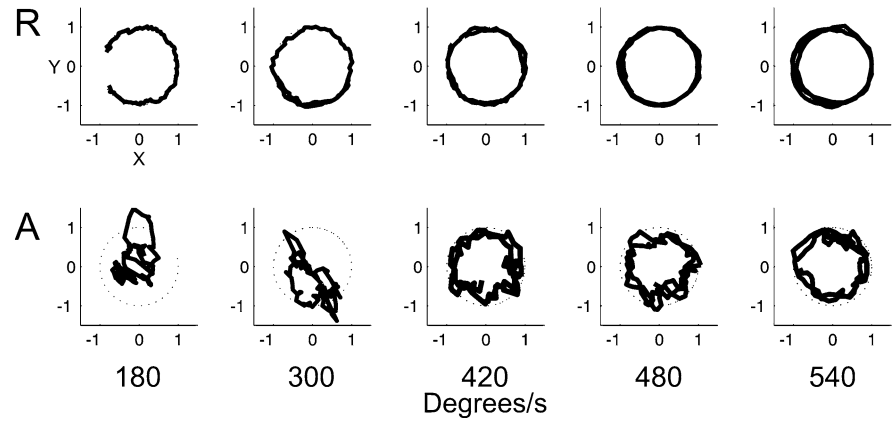
Real Motion

Apparent Motion

180   300   420   480   540

Stimulus Speed (degrees/s)

Fig. 4 Predicted stimulus position using an ensemble of ten neurons during the real (*R*) and apparent (*A*) motion conditions and for the five different stimulus speeds. The kernel size window was 300 ms, and the time shift was +20 ms

the quality of the reconstruction was speed-dependent. Next we examine more specific aspects of this finding.

Three main variables could be controlled to optimize the performance of the linear algorithm: the number of neurons included in the model, the kernel size, and the time lag between the stimulus position and the neural activity. Thus the first step was to estimate the minimum number of neurons necessary to produce an accurate stimulus position reconstruction. For this purpose a bootstrap technique was used in which the multiple

regression model was performed for a fixed number *k* of neurons taken randomly (without replacement) from the ensemble of 90 neurons. A total of 1000 repetitions for each population number were carried out. Figure 5 shows the R^2 cumulative distribution for linear models carried out using a cross-validation method in both motion conditions and for the different stimulus speeds. The highest fits were obtained using 10–15 neurons.

Next we estimated the best kernel size and the best time lag between the stimulus position and the activity of a
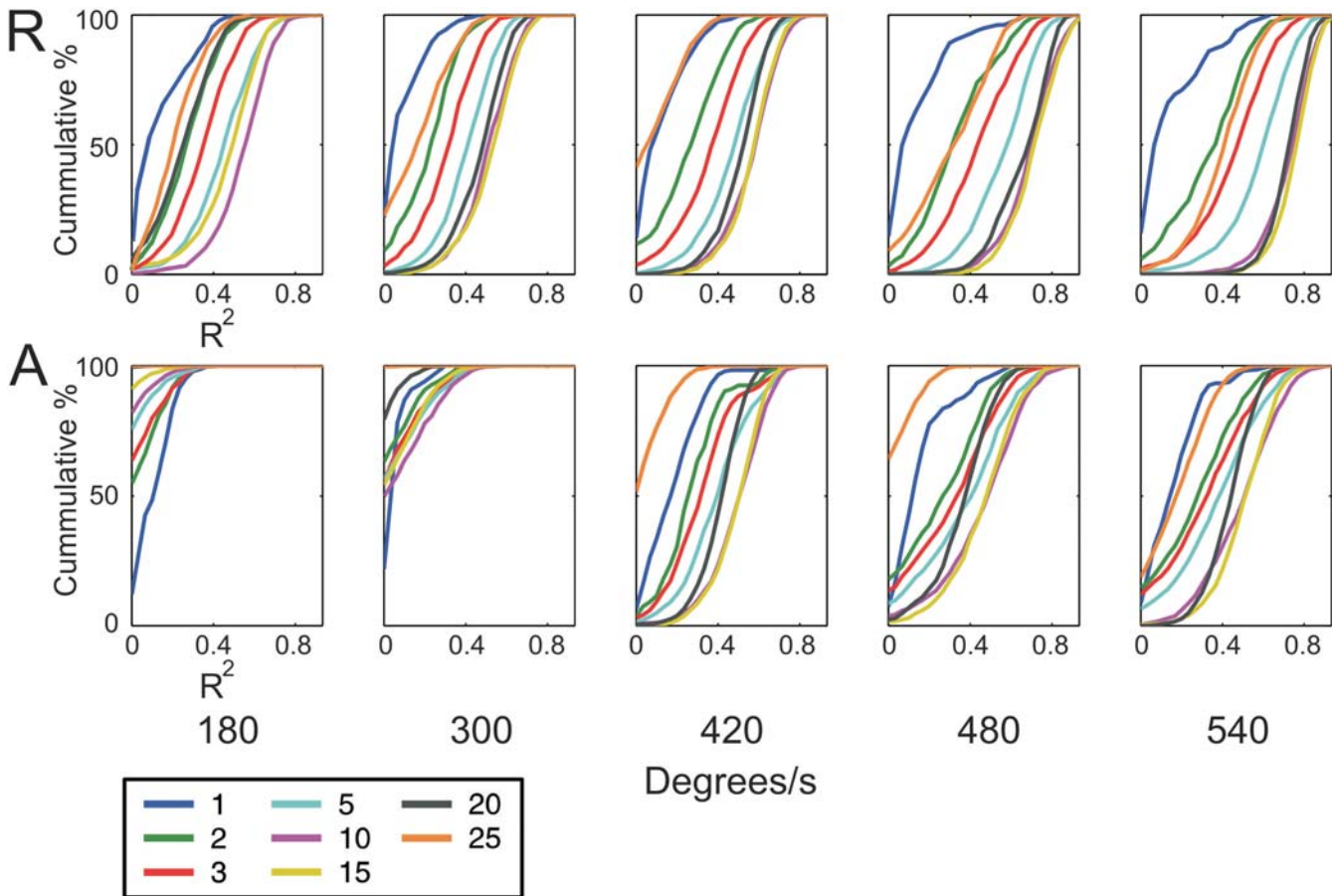

Fig. 5 Cumulative distributions of the R^2 of linear models carried out with different number of neurons, during both the real (*R*) and apparent (*A*) motion conditions and for different stimulus speeds.

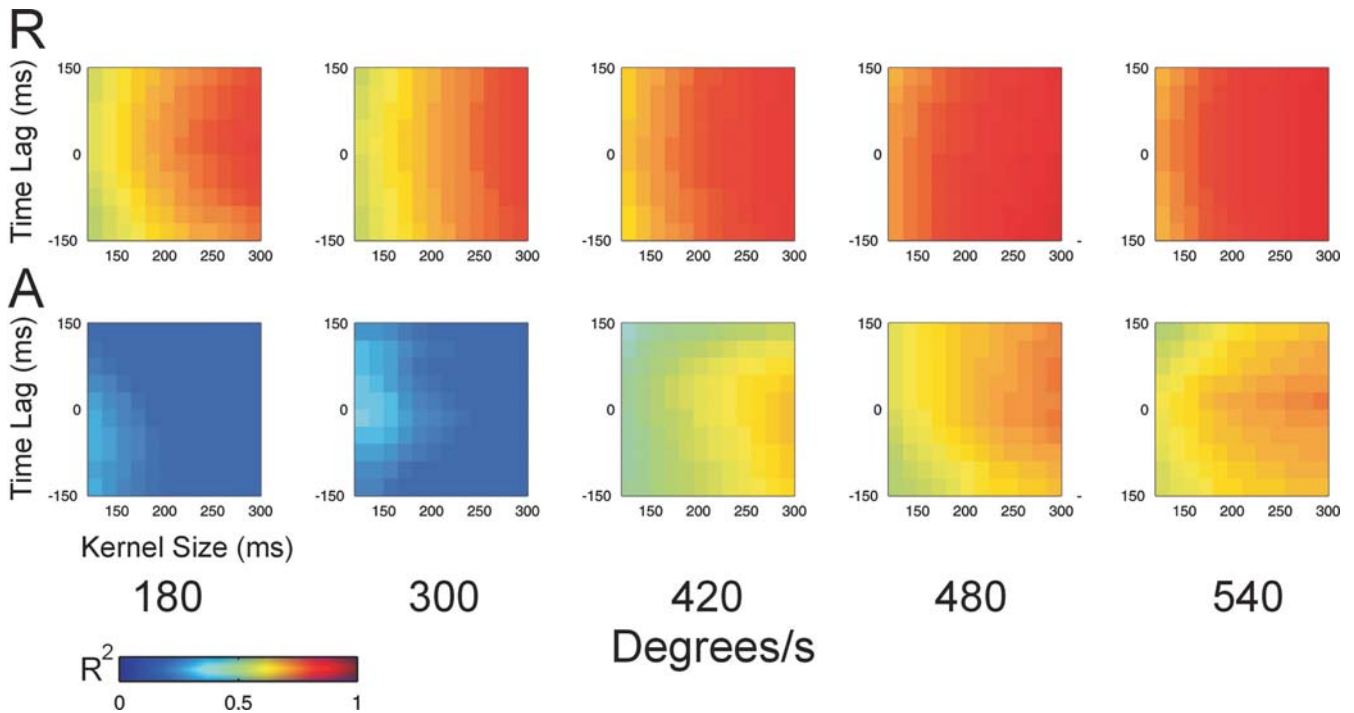The legend specifies the color-code for the different number of neurons used

Fig. 6 Values of R^2 in color scale for linear models performed in 20 neurons using different kernel durations and time lag between the stimulus position and the neural activity for the real (R) and apparent (A) motion conditions and different stimulus speeds

particular ensemble of 20 cells (Fig. 6) by varying these two parameters systematically. Three main results were obtained. First, the stimulus position reconstruction was adequate for real moving stimuli at all stimulus speeds tested. Second, the coding of stimulus position in apparent motion was speed-dependent. Only at stimulus speeds above 300°/s was the reconstruction of the linear models accurate (R^2 above 0.5). In fact poor coding was also was observed on the stimulus speeds of 180° and 300°/s in the apparent motion condition, when the relationship between the goodness of fit and ensemble size was determined (Fig. 5). Finally, the best fit was obtained at kernel sizes around 250 ms, and the best time shift between stimulus position and neural activity was around 0 ms.

The number of neurons and the kernel size are variables that define the complexity of the linear model. Although the optimization of these variables is important, the goodness of fit of the models is also influenced by the amount of data available (number of training trials and length of the time series). Therefore there is a trade-off between the degrees of freedom of the data available and the degrees of freedom of the parameters of the model. For example, a linear system analysis carried out on a data base with more and longer trials would probably achieve better fits than the obtained here with a more complex model (more neurons and longer kernels). Taking these statistical constraints into consideration, the best number of neurons and the kernel size reported in present study are optimized for the available data, and do not necessarily represent the "absolute" best.

Neural coding and psychophysics

We compared the psychometric curve of apparent motion detection (mean ±SD) as a function of the stimulus speed with the sigmoidal function obtained from R^2 values of the linear model during the apparent motion condition (Fig. 7). The two functions showed a very similar shape. The stimulus speed at detection threshold in human subjects was almost identical to the stimulus speed at half the maximum R^2 (314° and 320°/s, respectively). The R^2 (mean ±SD) values in this case were obtained from the 100 of 10,000 regression models with the highest fits. These models were tested on a set of 20 neurons which yielded the best results, using a kernel size of 150 ms and time lags that were randomly chosen for each neuron ranging from −240 to 180 ms, in steps of 60 ms. This analysis was performed with the purpose of taking into consideration the possibility that the response latencies of the neurons used were different. Nevertheless, the stimulus speed at half the maximum R^2 from an analysis using a kernel size of 270 ms and a lag of 0 ms was 334.8°/s. Finally, the coding performance for real motion stimulus was highly accurate for all the stimulus speeds (Fig. 7, diamonds).

Discussion

This study provides the first direct comparison between physiological and psychophysical responses to path-guided apparent motion. The detection of path-guided apparent motion in human subjects was tightly correlated
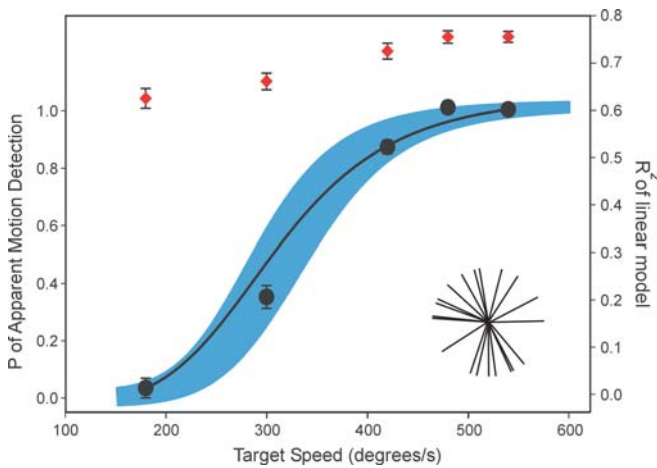
Fig. 7 Comparison between the psychometric curve of apparent motion detection as a function of the stimulus speed (mean ±SD, *blue lines*) with the sigmoideal function obtained from the R^2 (mean ±SD, n=100 of 10,000) from the 20 neurons with the highest fits, a kernel duration of 150 ms, and the best time lags of the lineal model during the apparent motion condition for the different stimulus speeds (*black circles*, *continuous line*). *Solid diamonds* The best R^2 (mean ±SD) of the lineal model during the real motion condition. *Inset* The preferred angular position for these 20 neurons

to the correct reconstruction of the stimulus position by ensembles of neurons in area 7a using a multivariate linear regression model. For both measures the performance followed similar S-shaped functions, with thresholds that were almost identical.

A fundamental problem in neuroscience is to determine how different aspects of behavior are represented by neurons in the CNS. In this sense a basic principle had been postulated: the information of variables is not encoded by single cells but rather by populations of neurons. For instance, a basic property of single cells is that they are tuned to a particular range of values of a variable or variables. Therefore a population of cells is needed to cover the entire extent of the parameter. Tuning has been observed in practically all the sensory modalities as well as in the motor and cognitive systems. Now the use of decoding techniques has made it possible to estimate the true value of an external variable on the basis of recording of spike data from tuned populations of cells. Various decoding procedures have been developed, including the population vector (Georgopoulos et al. 1986, 1989, 1992), the Bayesian, and the maximum likelihood inference methods (Dayan and Abbott 2002; Pouget et al. 2003). Decoding is a very useful approach to understand how the brain processes information to accomplish behavior through the interaction of neural populations. In the present study we used a spike-train decoding method to reconstruct a time-varying parameter: the position of the stimulus in time (Dayan and Abbott 2002; Humphrey et al. 1970; Wessberg et al. 2000). We used the decoded position of the stimuli as a signal that could reflect the perceptual capabilities of monkeys to detect PAM. This signal may reflect the ability of the posterior parietal cell populations to code circularly moving stimuli under real and apparent motion conditions.

Single cell encoding of real and apparent motion have been reported elsewhere (Merchant et al. 2004a).

The strategy of combing psychophysical and neurophysiological data, pioneered by Mountcastle and collaborators in the 1960s and 1970s (LaMotte and Mountcastle 1975; Mountcastle et al. 1972; Talbot et al. 1968), has proved a very fruitful approach in the study of perception in all sensory modalities (Parker and Newsome 1998). The similarity in the psychometric performance in humans and in nonhuman primates has justified this type of comparison. With respect to stimulus motion it has been shown that the perception of motion in monkeys is similar to that of humans (De Valois and Morgan 1974; De Valois et al. 1974; Golomb et al. 1985; Merchant et al. 2003a). Therefore it is reasonable to suppose that the detection threshold of path-guided apparent motion in monkeys is similar to the detection threshold in human subjects quantified here. Indeed, direct correlations between the physiological and psychophysical responses in the same monkey have been reported recently with great success in tactile and visual motion discrimination and categorization tasks (Britten et al. 1992; Hernandez et al. 2000; Merchant et al. 1997).

The present results suggest that an explicit visual representation of a moving stimulus changing dynamically in the perceived circular path of motion is created by ensembles of neurons in area 7a during the apparent motion condition. This dynamic representation is similar to the one observed with real circularly moving stimuli only when the spatiotemporal characteristics of the apparent motion stimuli produce a compelling perception of path-guided apparent motion. It has been shown that neurons in area 7a respond to visual motion, including complex stimuli such as optic flow (Merchant et al. 2001, 2003b; Siegel and Read 1997). In addition, these cells have large receptive fields and are modulated by the attentional load of the visual stimuli (Constantinidis and Steinmetz 2001; Motter and Mountcastle 1981). Thus these properties indicate that a high degree of convergence and integration of visual motion information is taking place in this area, which make area 7a a structure well suited to represent a high-level stimulus such as path-guided apparent motion. Indeed, the present results support the late cortical locus model for perceptual filling-in during path-guided apparent motion (Liu et al. 2004). It has been suggested that the perception of apparent moving stimuli depends on a high-level system that includes the parietal cortex and depends on attention mechanisms (Cavanagh 1992; Battelli et al. 2001; Lu and Sperling 2001; Sterzer et al. 2002). Psychophysical experiments indicated that the high-level system is based on position signals (Lu and Sperling 2001; Seiffert and Cavanagh 1998), and that it is different from a low level system that is passive, effortless and based on velocity changes. Thus the coding of the stimulus position over time by populations of cells in area 7a could be an explicit neural mechanism for high-level motion perception.

We have demonstrated that neurons in area 7a are involved in the interception of real and path-guided

apparent moving stimuli, and that the stimulus position can be used to trigger the interception movement (Merchant et al. 2004b). Therefore the dynamical coding of the perceived circular trajectory of the stimulus by cell ensembles in area 7a is not only a possible neural mechanism for apparent motion perception but also a signal that can be used to drive the behavior towards or away from the perceptual representation of a moving object.

References

Andersen RA, Asanuma C, Essick G, Siegel RM (1990) Corticocortical connections of anatomically and physiologically defined subdivisions within the inferior parietal lobule. J Comp Neurol 296:65–113

Anstis SM (1980) The perception of apparent movement. Philos Trans R Soc Lond B Biol Sci 290:153–168

Battelli L, Cavanagh P, Intriligator J, Tramo MJ, Henaff MA, Michel F, Barton JJ (2001) Unilateral right parietal damage leads to bilateral deficit for high-level motion. Neuron 32:985–995

Britten KH, Shadlen MN, Newsome WT, Movshon JA (1992) The analysis of visual motion: a comparison of neuronal and psychophysical performance. J Neurosci 12:4745–4765

Cavanagh P (1992) Attention-based motion perception. Science 257:1563–1565

Chatterjee SH, Freyd JJ, Shiffrar M (1996) Configural processing in the perception of apparent biological motion. J Exp Psychol Hum Percept Perform 22:916–929

Constantinidis C, Steinmetz MA (2001) Neuronal responses in area 7a to multiple-stimulus displays. I. neurons encode the location of the salient stimulus. Cereb Cortex 11:581–591

Dayan P, Abbott LF (2002) Theoretical neuroscience: computational and mathematical modeling of neural systems. MIT Press, Cambridge

De Valois R, Morgan HC (1974) Psychophysical studies of monkey vision. II. Squirrel monkey wavelength and saturation discrimination. Vision Res 14:69–73<1

De Valois RL, Morgan HC, Polson MC, Mead WR, Hull EM (1974) Psychophysical studies of monkey vision. I. Macaque luminosity and color vision tests. Vision Res 14:53–67

Felleman DJ, Van Essen DC (1991) Distributed hierarchical processing in the primate cerebral cortex. Cereb Cortex 1:1–47

Georgopoulos AP, Schwartz AB, Kettner RE (1986) Neuronal population coding of movement direction. Science 233:1416–1419

Georgopoulos AP, Lurito JT, Petrides M, Schwartz AB, Massey JT (1989) Mental rotation of the neuronal population vector. Science 243:234–236

Georgopoulos AP, Ashe J, Smyrnis N, Taira M (1992) Motor cortex and the coding of force. Science 256:1692–1695

Golomb B, Andersen RA, Nakayama K, MacLeod DI, Wong A (1985) Visual thresholds for shearing motion in monkey and man. Vision Res 25:813–820

Hernandez A, Zainos A, Romo R (2000) Neuronal correlates of sensory discrimination in the somatosensory cortex. Proc Natl Acad Sci U S A 97:6191–6196

Humphrey DR, Schmidt EM, Thompson WD (1970) Predicting measures of motor performance from multiple cortical spike trains. Science 170:758–762

Kolers PA (1972) Aspects of motion perception. Pergamon, New York

LaMotte RH, Mountcastle VB (1975) Capacities of humans and monkeys to discriminate vibratory stimuli of different frequency and amplitude: a correlation between neural events and psychological measurements. J Neurophysiol 38:539–559

Liu T, Slotnick SD, Yantis S (2004) Human MT+ mediates perceptual filling-in during apparent motion. Neuroimage 21:1772–1780

Lu ZL, Sperling G (2001) Three-systems theory of human visual motion perception: review and update. J Opt Soc Am A Opt Image Sci Vis 18:2331–2370

Merchant H, Zainos A, Hernandez A, Salinas E, Romo R (1997) Functional properties of primate putamen neurons during the categorization of tactile stimuli. J Neurophysiol 77:1132–1154

Merchant H, Battaglia-Mayer A, Georgopoulos AP (2001) Effects of optic flow in motor cortex and area 7a. J Neurophysiol 86:1937–1954

Merchant H, Battaglia-Mayer A, Georgopoulos AP (2003a) Interception of real and apparent motion targets: psychophysics in humans and monkeys. Exp Brain Res 152:106–112

Merchant H, Battaglia-Mayer A, Georgopoulos AP (2003b) Functional organization of parietal neuronal responses to optic flow stimuli. J Neurophysiol 90:675–682

Merchant H, Battaglia-Mayer A, Georgopoulos AP (2004a) Neural responses in motor cortex and area 7a to real and apparent motion. Exp Brain Res 154:291–307

Merchant H, Battaglia-Mayer A, Georgopoulos AP (2004b) Neural responses during interception of real and apparent circularly moving targets in Motor Cortex and Area 7a. Cereb Cortex 14:314–331

Mikami A (1991) Direction selective neurons respond to short-range and long-range apparent motion stimuli in macaque visual area MT. Int J Neurosci 61:101–112

Motter BC, Mountcastle VB (1981) The functional properties of the light-sensitive neurons of the posterior parietal cortex studied in waking monkeys: foveal sparing and opponent vector organization. J Neurosci 1:3–26

Mountcastle VB, LaMotte RH, Carli G (1972) Detection thresholds for stimuli in humans and monkeys: comparison with threshold events in mechanoreceptive afferent nerve fibers innervating the monkey hand. J Neurophysiol 35:122–136

Muckli L, Kriegeskorte N, Lanfermann H, Zanella FE, Singer W, Goebel R (2002) Apparent motion: event-related functional magnetic resonance imaging of perceptual switches and states J Neurosci 22:RC219

Newsome WT, Mikami A, Wurtz RH (1986) Motion selectivity in macaque visual cortex III Psychophysics and physiology of apparent motion. J Neurophysiol 55:1340–1351

Parker AJ, Newsome WT (1998) Sense and the single neuron: probing the physiology of perception. Annu Rev Neurosci 21:227–277

Pouget A, Dayan P, Zemel RS (2003) Inference and computation with population codes. Annu Rev Neurosci 26:381–410

Ramachandran VS, Anstis SM (1983) Perceptual organization in moving patterns. Nature 304:529–531

Seiffert AE, Cavanagh P (1998) Position displacement, not velocity, is the cue to motion detection of second-order stimuli Vision Res 38:3569–3582

Shepard RN (1984) Ecological constraints on internal representation: resonant kinematics of perceiving, imagining, thinking, and dreaming. Psychol Rev 91:417–447

Shepard RN, Zare SL (1983) Path-guided apparent motion. Science 220:632–634

Siegel RM, Read HL (1997) Analysis of optic flow in the monkey parietal area 7a. Cereb Cortex 7:327–346

Sterzer P, Russ MO, Preibisch C, Kleinschmidt A (2002) Neural correlates of spontaneous direction reversals in ambiguous apparent visual motion. Neuroimage 15:908–916

Talbot WH, Darian-Smith I, Kornhuber HH, Mountcastle VB (1968) The sense of flutter-vibration: comparison of the human capacity with response patterns of mechanoreceptive afferents from the monkey hand. J Neurophysiol 31:301–334

Wessberg J, Stambaugh CR, Kralik JD, Beck PD, Laubach M, Chapin JK, Kim J, Biggs SJ, Srinivasan MA, Nicolelis MA (2000) Real-time prediction of hand trajectory by ensembles of cortical neurons in primates. Nature 408:361–365

Williams ZM, Elfar JC, Eskandar EN, Toth LJ, Assad JA (2003) Parietal activity and the perceived direction of ambiguous apparent motion. Nat Neurosci 6:616–623

Yantis S, Nakama T (1998) Visual interactions in the path of apparent motion. Nat Neurosci 1:508–512